ACS OMEGA

http://pubs.acs.org/journal/acsodf

Article

# Effects of Initial Turbulence on the Explosion Limit and Flame Propagation Behaviors of Premixed Syngas−Air Mixtures

Huarong Zhang, Yingxin Tan,* Shuo Zhang, Yabei Xu, Yuxin Zhao, Jiaxin Guo, and Weiguo Cao*

Cite This: *ACS Omega* 2021, 6, 30910−30918

Read Online

ACCESS | Metrics & More | Article Recommendations

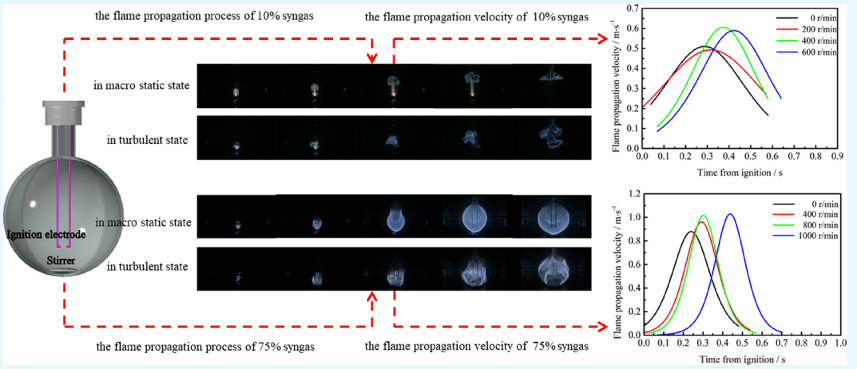


**ABSTRACT:** Syngas with important industrial applications has explosive hazards because of its flammability. It is necessary and valuable to study the combustion and explosion characteristics of syngas under actual working conditions. To explore the effects of initial turbulence on the explosion limits and the flame propagation behavior of the syngas−air mixtures, the explosion limits were tested by the explosive limit instrument, and the flame propagation process in the spherical pressure vessel was recorded by a high-speed camera. By adjusting the rotating speed of the stirrer to obtain turbulence of different intensities, the explosion limit and flame propagation behavior of syngas under different turbulent conditions were analyzed. The explosion limit of syngas in the macro-static state was 9.5−76.1%, and its flame front was relatively smooth. However, with the increase in turbulence intensity, both the upper and lower explosion limits of syngas decreased. The disturbance of turbulence made the flame shape change. The flame front was wrinkled, and the flame boundary was blurred, which became more and more obvious with the increase in turbulence intensity. The maximum velocity and duration of flame propagation increased with the increase in turbulence intensity. Under the same turbulence intensity, the flame propagation velocity generally augmented first and then lessened.

## 1. INTRODUCTION

With the increasing demand for energy and people's concern for environmental protection, the research on clean alternative power system has attracted more and more attention in recent years. In these studies, the integrated gasification combined cycle (IGCC) technology can achieve higher efficiency and lower emissions, which is the most promising clean and efficient coal power technology in the world.[1,2] The IGCC power plant gasifies various carbonaceous solid fuels (coal, biomass, and solid waste) into a syngas mixture for use in gas turbines to generate electricity.[3−5] The syngas can also be used as fuel for other combustion devices, such as internal combustion engines or cookers.[6] Syngas can not only improve the efficiency of energy utilization but also significantly reduce the emission of pollutants, which has a salient development prospect in the production and use of clean energy.

The main components of syngas are CO and $H_2$, which may contain small amounts of $CO_2$, $N_2$, $H_2O$, and $CH_4$.[7−10] The specific composition of syngas depends on fuel resources and processing conditions, which has great variability. There are a lot of diluents ($CO_2$ and $N_2$) in the composition of biomass-derived syngas.[11] This variability has a great influence on the fuel performance and combustion process and is a major challenge in the design of combustion chambers. In recent years, syngas has been widely used in power generation, transportation, and other fields.[12−14] However, as a kind of combustible mixed gas, syngas is prone to combustion and explosion once it leaks in the process of production, storage, transportation, and use.[15−18] Therefore, to ensure the safety of syngas in industrial production and use, it

Received: May 26, 2021
Accepted: October 27, 2021
Published: November 9, 2021

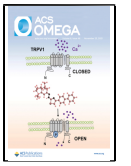

is extremely important to understand the combustion and explosion characteristics of syngas.

At present, scholars have accomplished plenty of research studies on the combustion characteristics of syngas, such as the combustion mechanism,[19] laminar flame velocity,[20−25] flammability limit, and extinction limit.[26] The research results of combustion characteristics of syngas have important reference values for mastering the explosion characteristics of syngas. Tran et al.[27] analyzed the explosion characteristics of syngas in a cylindrical container through experiments and numerical simulations and acquired the change rule of explosion pressure under different hydrogen volume fractions and different equivalence ratios. Liu et al.[28] studied the effect of $CO_2$ and $H_2O$ on the explosion limit of syngas, and the influencing factors and mechanism had been analyzed and discussed. Sun[29] explored the laminar explosion behavior of syngas in a spherical container and obtained the temporal traces of explosion overpressure and the variations of four essential explosion indices (maximum explosion pressure, explosion duration, peak pressure rise rate, and deflagration index) under different fuel concentrations and hydrogen volume. Some scholars have focused on the explosion characteristics of syngas. Most of the research on the explosion characteristics of syngas focuses on the explosion overpressure, and there are few reports on the flame propagation structure and flame propagation speed during the explosion process. Therefore, it is necessary to further study the explosion characteristics of syngas.

Numerous of scholars have conducted plenty of research studies on laminar premixed combustion of syngas. However, most of the combustion and explosion processes are carried out in turbulent environments, especially the combustion of power equipment. Therefore, it is of great practical significance to explore the effect of turbulence on the explosion limit and flame propagation process of syngas. Turbulence affects both the ignition and explosion characteristics of combustible gases.[30,31] In the occurrence and development of combustible gas explosions, turbulence can be divided into two categories according to the different causes of formation: (1) initial turbulence, the turbulence that already exists before the combustible mixture ignites, and (2) explosion-induced turbulence, the turbulence generated by the explosion itself, such as the turbulence caused by obstacles, sudden changes in the cross section of the duct, and wall roughness during the flame propagation process.[32] The influence of explosion-induced turbulence on the flame propagation of combustible gas was well studied worldwide. Wang et al.[33] conducted an experimental analysis on the deflagration flame propagation of premixed methane−air gas in a closed channel containing different obstacles. The results showed that extremely complex changes occurred when the deflagration flame passed through obstacles of different shapes in the closed channel, and the obstacles in the channel enhanced the propagation of the deflagration flame to the unburned area. Wang et al.[34] studied the influence of different configurations of variable cross section ducts on the flame structure, flame propagation speed, and overpressure of hydrogen/methane/air premixed gas. The results delineated that when the cross section changed suddenly and the smooth flame front folded and formed a turbulent flame. Starr et al.[35] studied the detonation limits of rough-walled tubes and found that the detonation limits in rough-walled tubes were wider than those in smooth tubes. This depicted that the turbulence generated by the wall roughness promoted the propagation of detonation and extended the limits.

The effect of initial turbulence on the explosion limit and flame propagation of combustible gas had also been preliminarily explored by scholars. Bauwens et al.[36] studied the influence of different turbulence intensity on the explosion behavior of hydrogen−air mixtures and found that the strengthening of the initial turbulence increased the overall propagation speed of the flame, and this increase in speed was converted to a higher peak overpressure during the external explosion process. Bai et al.[37] studied the effect of initial turbulence on the typical explosion characteristics of methane−air mixtures with different concentrations. The results clearly showed that turbulence had a significant enhancement effect on the explosion, and the influence of jet turbulence on $P_{max}$ was more significant near the flammability limit than under the stoichiometric condition. Sun et al.[38] conducted a vented explosion test of a methane−air mixture to study the effect of concentration and initial turbulence on the pressure characteristics and flame development. The initial turbulence deformed the flame front, significantly increased the peak pressure, and stimulated the generation of acoustic oscillation at the upper and lower limits of concentration.

In summary, most of the current research studies on the explosion limit and flame propagation of combustible gas in a turbulent state was the influence of explosion-induced turbulence on the flame propagation process. The research on the effect of initial turbulence on the explosion process of explosive mixture mainly focused on combustible dust[39−43] and rarely involved combustible gas. For syngas, most of the current research focused on combustion characteristics but few on the explosion characteristics of syngas. Therefore, the influence of turbulence on the explosion limit and flame propagation process of syngas was studied in this paper. This study aimed to supplement the existing research and provide a reference for the analysis of the development mechanism of syngas explosion.

## 2. RESULTS AND DISCUSSION

**2.1. Effect of Turbulence on the Explosion Limit.** The explosion limit data of pure gas can be obtained directly from the database (room temperature and atmospheric pressure). For a mixture of two or more flammable gases or vapors, the explosion limit can be calculated according to the Le Chatelier Formula. The calculation formula eq 1 is as follows:

$$L_m = \frac{1}{\sum_{i=1}^{n} \frac{\chi_i}{L_i}} \tag{1}$$

where $L_m$ is the explosion limit of gaseous mixture, $L_i$ is the explosion limit of one component in the gaseous mixture, $x_i$ is volume fraction of one component in the gaseous mixture, and $n$ is number of the components.

For the mixture of flammable gas and inert gas, the explosion limit can be calculated by eq 2:

$$L'_m = L_m \times \frac{\left(1 + \frac{B}{1-B}\right) \times 100}{100 + L_m \times \frac{B}{1-B}}\% \tag{2}$$

where $L'_m$ is the explosion limit of gaseous mixture with inert gases and $B$ is the volume fraction of the inert gases.

For the syngas used in this experiment, the explosion limit was calculated by the above two formulas to be 7.463−78.468%.

The explosion limits of syngas in the macro-static state and turbulent state were tested in the experiment. The gas flow state was changed by adjusting the speed of the stirrer inside the



https://doi.org/10.1021/acsomega.1c02513
ACS Omega 2021, 6, 30910−30918

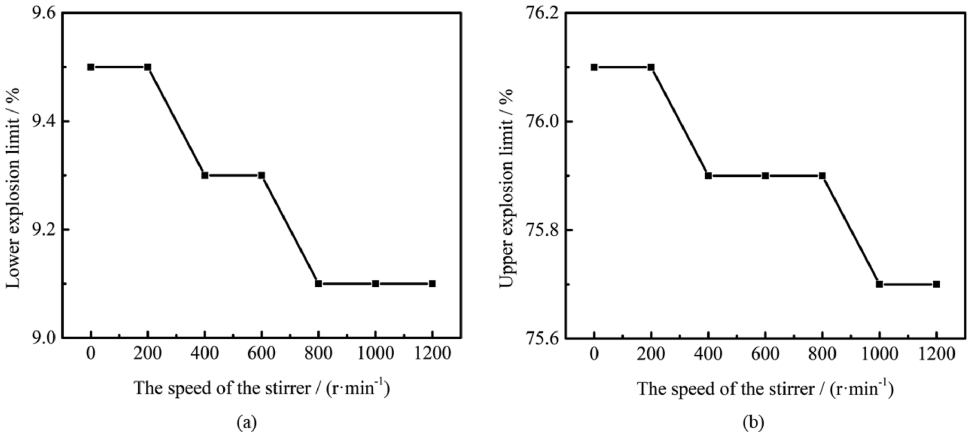


**Figure 1.** Effect of turbulence on the explosion limit of syngas: (a) lower explosion limit and (b) upper explosion limit.

instrument. The turbulence intensity of the mixed gas was characterized by the speed of the stirrer. During the test, a certain concentration of syngas−air mixture was injected into the reaction chamber and placed at a certain rotating speed for 5.0 min. In the process of the mixed gas flowing with the rotation of the stirrer, the combined effect of the inertia of the motion and the molecular viscosity would eventually lead the synthesis gas−air mixture in the reaction chamber to be in a turbulent state during ignition.

This study took the $CO/H_2/N_2$−air mixture as the research object and tested its explosion limit at different speeds (0, 200.0, 400.0, 600.0, 800.0, 1000.0, and 1200.0 r/min) to study the influence of turbulence on its explosion limit.

The explosion limit of syngas in the macro-static state measured by the test was 9.5−76.1%, and the calculated explosion limit was 7.463−78.468%. Compared with the calculated value, the explosion range of the experimental value was reduced. There are three main reasons for this error. First, the complex gas composition may be the reason behind the error. Second, only the composition and volume fraction of combustible gas are considered in the theoretical calculation formula, but the influence of factors such as bond energy, incomplete combustion, and decomposition of combustion products is ignored. The last possible reason is different test equipment. The explosion limit of combustible gas is affected by many factors, among which the shape, size, material, and other factors of the test container will affect the explosion limit. Due to the combined effect of the above factors, there was an error between the theoretical calculation results and the experimental data.

According to the test data, the relationship between the explosion limit and turbulence intensity is drawn, as listed in Figure 1.

It can be seen from Figure 1a that the lower explosion limit of syngas decreased with the increase in rotating speed (turbulence intensity). When the rotating speed was 0−200.0 r/min, the lower explosion limit was 9.5%, which was the same as the lower explosion limit of the mixed gas in the macro-static state. When the rotating speed was 200.0−400.0 r/min, the lower explosion limit decreased from 9.5 to 9.3%. When the rotating speed was 600.0−800.0 r/min, the lower explosion limit decreased from 9.3 to 9.1%. When the rotating speed was 800.0−1200.0 r/min, the lower explosion limit was the lowest, 9.1%. The analysis shows that the initial turbulence enhances the heat and mass transport between the flame and the unburned gas. In the process of flame propagation, heat transfer means that the heat in the burned area will be carried to the unburned area, and then the heat of the flame will be lost and the temperature will be reduced, which will inhibit the flame propagation. Mass transfer means that the fuel and oxygen in the unburned area will be brought into the reaction zone, so the chemical reaction will be maintained and the flame propagation will be promoted. For flame propagation near the lower explosion limit, the mass transfer process plays a major role in controlling. Under the influence of the turbulent field, the mass transfer process is greatly enhanced, while the heat loss in the heat transfer process is negligible. Therefore, the progress of the chemical reaction is promoted, which is manifested as a decrease in the lower explosion limit.

It can be seen from Figure 1b that with the increase in rotating speed (turbulence intensity), the upper explosion limit of syngas also decreased. When the rotating speed was 0−200.0 r/min, the upper explosion limit was 76.1%, which was the same as that in the macro-static state. When the rotating speed was 400.0−800.0 r/min, the upper explosion limit was 75.9%. With the speed increased to 1000.0 r/min, the upper explosion limit was reduced from 75.9 to 75.7%. This is because in the flame propagation process near the upper explosion limit, the heat transfer process plays a major controlling role. Under the effect of turbulence, the heat transfer process is strengthened, the flame heat loss is increased, and the flame propagation is suppressed, which is manifested by the decrease in the upper explosion limit.

**2.2. Flame Propagation Process of Syngas in the Macro-static State.** A high-speed camera was used to record the entire process of flame propagation in the spherical combustion chamber. The flame pictures at a certain interval during the ignition process were selected to measure the height of the flame front at the corresponding moment using Photoshop software. The relationship curve between the flame front and time was fitted out with a continuous curve equation, and then the instantaneous velocity of flame propagation at each moment was obtained by calculating the first-order derivative of the curve.

Figure 2 depicts the flame propagation process of the syngas with a concentration of 10% in a spherical container in the macro-static state (0 r/min). The spark ignition moment was 0 ms. At this time, the high-voltage electrode discharged, and a strong blue-white light group was generated around the electrode. At 40.0 ms, the cluster agglomerated, the fuel ignited,


https://doi.org/10.1021/acsomega.1c02513
ACS Omega 2021, 6, 30910−30918

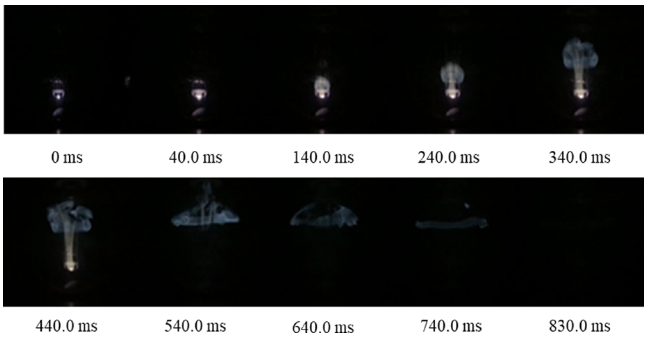


**Figure 2.** Pictures of the flame propagation process of 10.0% syngas (macro-static state).

and the flame shape was spherical. After the mixed gas was ignited, the flame propagation speed was slow in the initial stage, and the spherical flame slowly expanded and continued to expand and extend. At 340.0 ms, the brightness of the combustion zone was strong, and it was a blue flame. With the continuation of the ignition time, the flame propagation speed gradually accelerated. The flame expanded freely around from the ignition position to the vessel wall, and the height of the flame front reached the maximum at about 500.0 ms. The concentration of syngas gradually decreased with the progress of the combustion reaction, and the flame speed gradually decreased and was completely extinguished at 830.0 ms.

Different concentrations of syngas−air mixture were selected to conduct experiments to analyze the influence of concentration changes on flame propagation. Five concentrations of syngas (10.0, 10.5, 11.0, 11.5, and 12.0%) were selected for the experiment to study the flame propagation process near the lower explosion limit. Five concentrations of syngas (73.5, 74.0, 74.5, 75.0, and 75.5%) were selected for the experiment to study the flame propagation process near the upper explosion limit. By observing the pictures of flame propagation process, the time parameter records of flame propagation process of syngas with 10 concentrations were obtained, as showcased in Tables 1 and

**Table 1. Table of the Time Parameters of the Flame Propagation Process (near the Lower Explosion Limit)**

| concentration (%) | time for the flame to reach its maximum (ms) | flame duration (ms) |
|---|---|---|
| 10.0 | 500.0 | 790.0 |
| 10.5 | 420.0 | 1280.0 |
| 11.0 | 410.0 | 1120.0 |
| 11.5 | 370.0 | 1110.0 |
| 12.0 | 360.0 | 1090.0 |

2. Table 1 delineates that near the lower explosion limit, as the concentration increased, the time for the flame to reach its maximum abated, and the duration of the flame became shorter. It can be seen from Table 2 that near the upper explosion limit, as the concentration increased, the time for the flame to reach the maximum increased, and the duration of the flame became longer.

**Table 2. Table of the Time Parameters of the Flame Propagation Process (near the Upper Explosion Limit)**

| concentration (%) | time for the flame to reach its maximum (ms) | flame duration (ms) |
|---|---|---|
| 73.5 | 200.0 | 330.0 |
| 74.0 | 330.0 | 530.0 |
| 74.5 | 330.0 | 530.0 |
| 75.0 | 460.0 | 730.0 |
| 75.5 | 490.0 | 760.0 |

Through the analysis of the test data, the curves of the flame front and flame propagation velocity of the syngas near the lower explosion limit (at the explosion concentrations of 10.0, 10.5, 11.0, 11.5, and 12.0%) were received, as shown in Figures 3 and

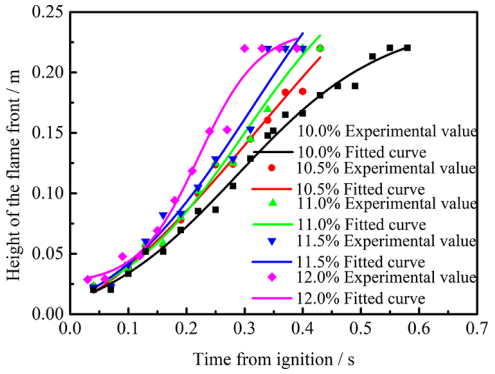


**Figure 3.** Variation of the height of the flame front with different concentrations (near the lower explosion limit).

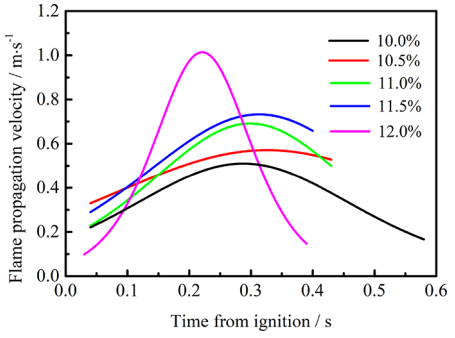


**Figure 4.** Variation of flame propagation speed with different concentrations (near the lower explosion limit).

4. The flame front of syngas reached the maximum height at 500.0, 420.0, 410.0, 370.0, and 360.0 ms, and the flame speeds reached their maximum at 286.0, 326.0, 298.0, 312.0, and 221.0 ms after ignition, which were 0.510, 0.571, 0.691, 0.733, and 1.014 m/s, respectively.

Figures 5 and 6 show the curves of the flame front and flame propagation velocity of the syngas at different concentrations near the upper explosion limit (at the explosion concentrations of 73.5, 74.0, 74.5, 75.0, and 75.5%). It can be seen from the figures that the flame front of syngas reached the maximum height at 200.0, 330.0, 330.0, 460.0, and 490.0 ms, and the flame speeds reached their maximum at 104.0, 170.0, 190.0, 239.0, and 277.0 ms after ignition, which were 1.962, 1.743, 1.630, 0.879, and 0.840 m/s respectively.

It can be seen from the analysis of the test results that in the macro-static state, the flame propagates at a lower speed for a period of time, then increases rapidly to the maximum value, and finally decreases gradually. Near the lower explosion limit, as the concentration of syngas increases, the flame propagation speed increases, and the flame duration becomes shorter. Near the


https://doi.org/10.1021/acsomega.1c02513
ACS Omega 2021, 6, 30910−30918

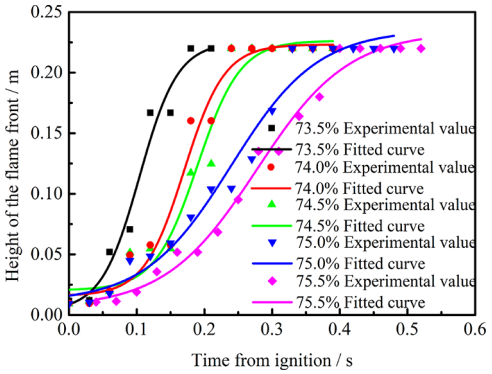


**Figure 5.** Variation of the height of the flame front with different concentrations (near the upper explosion limit).

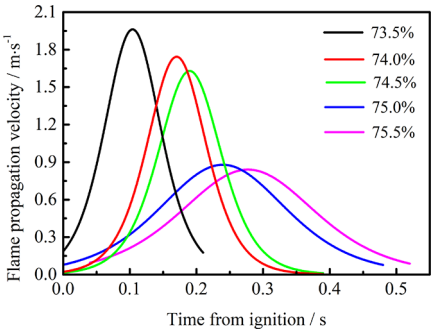


**Figure 6.** Variation of flame propagation speed with different concentrations (near the upper explosion limit).

upper explosion limit, as the concentration of syngas increases, the flame propagation speed decreases, and the flame duration becomes longer. When the concentration of the mixture is near the lower explosion limit, the air content is relatively excessive, and the combustible gas content is relatively insufficient. With the increase in syngas concentration, more flammable gas reacts with oxygen molecules, and the reaction rate increases rapidly. Compared with the lower explosion limit, the mixture contains excessive combustible gas and relatively insufficient air content near the upper explosion limit. As the concentration of syngas gradually increases, the oxygen content participating in the reaction gradually decreases, which leads to the decrease in the reaction speed. In particular, the reason why the flame duration of syngas with a concentration of 10.0% was less than 10.5% was because although its flame propagation speed was less than 10.5%, its fuel was less, so the flame duration was short.

**2.3. Effect of Turbulence on Flame Propagation.** The influence of turbulence on flame propagation near the explosion limit of syngas was studied experimentally. The syngas−air mixtures with volume fractions of 10.0 and 75.0% were selected as the research objects, and the flame propagation process of the mixtures at different rotating speeds was studied.

Figure 7 shows the flame propagation process of syngas with a concentration of 10.0% in a spherical container under turbulent flow (600.0 r/min) captured by a high-speed camera. The spark ignition moment was 0 ms. At this time, the high-voltage electrode discharged, and a strong blue-white light cluster was generated around the electrode. At 70.0 ms, the light cluster agglomerated, the fuel ignited, and the flame shape was irregular. After the mixture was ignited, the front of the flame displayed obvious folds under the disturbance of turbulence, which was different from the smoother front under the macro-static state.

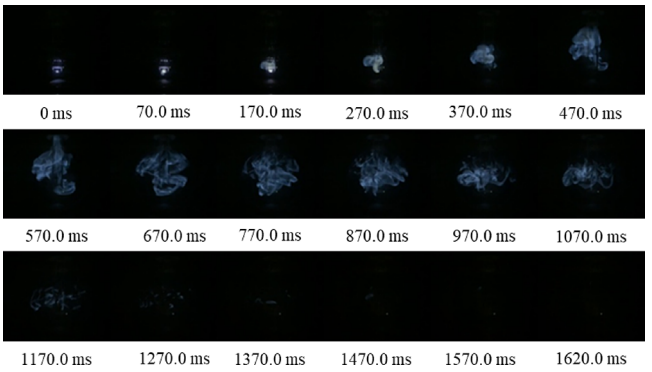


**Figure 7.** Pictures of the flame propagation process of 10.0% syngas (600.0 r/min).

In the initial stage, the flame propagation speed was slow. With the continuation of the ignition time, the flame propagation speed gradually accelerated. From the ignition position to the container wall, the flame expanded freely to the surroundings, the degree of wrinkles deepened, and the boundary was slightly unclear. The spherical flame reached its maximum at about 560 ms. With the combustion going on, the concentration of syngas gradually decreased, the flame luminescent zone gradually shrunk to the ignition end, and the flame speed gradually decreased and was completely extinguished at 1620.0 ms. The flame duration was longer than 790.0 ms at 0 r/min.

By observing the pictures of the flame propagation process of the syngas−air mixture at the same time but at different rotating speeds, it was found that the spherical flame front was smoother in the macro-static state. When the rotating speed increased, the folds of the spherical flame front were strengthened and the flame duration was longer.

Four rotating speeds of 0, 200.0, 400.0, and 600.0 r/min were chosen to test the flame propagation process of syngas with a concentration of 10.0%, and four rotating speeds of 0, 400.0, 800.0, and 1000.0 r/min were chosen to test the flame propagation process of syngas with a concentration of 75.0%. By observing the flame propagation process pictures, the time parameter tables of the syngas flame propagation process at four rotating speeds were obtained, as listed in Tables 3 and 4. With the increase in rotating speed, the time for the flame to reach its maximum increased, and the flame duration became longer.

**Table 3. Table of the Time Parameters of the Flame Propagation Process (10.0%)**

| speed of the stirrer (r/min) | time for the flame to reach its maximum (ms) | flame duration (ms) |
|---|---|---|
| 0 | 500.0 | 790.0 |
| 200.0 | 500.0 | 1090.0 |
| 400.0 | 560.0 | 1050.0 |
| 600.0 | 560.0 | 1550.0 |

**Table 4. Table of the Time Parameters of the Flame Propagation Process (75.0%)**

| speed of the stirrer (r/min) | time for the flame to reach its maximum (ms) | flame duration (ms) |
|---|---|---|
| 0 | 460.0 | 730.0 |
| 400.0 | 500.0 | 760.0 |
| 800.0 | 490.0 | 760.0 |
| 1000.0 | 630.0 | 860.0 |



https://doi.org/10.1021/acsomega.1c02513
ACS Omega 2021, 6, 30910−30918

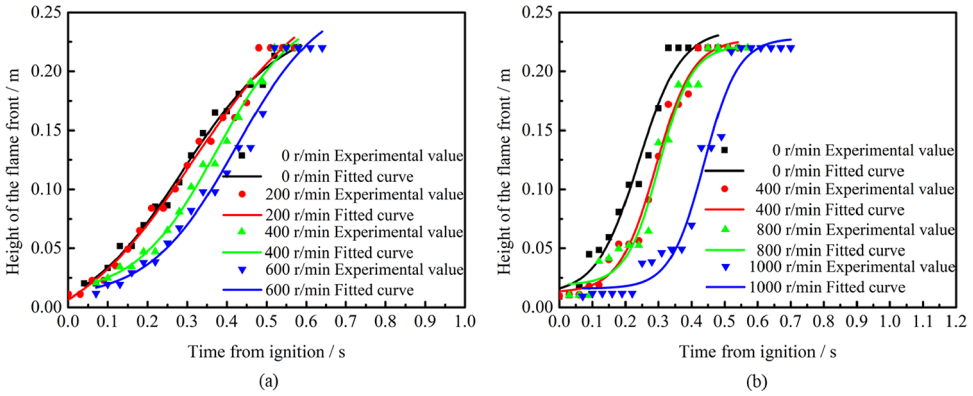


**Figure 8.** Variation of the height of the flame front with different speeds of the stirrer: (a) l0.0% and (b) 75.0%.

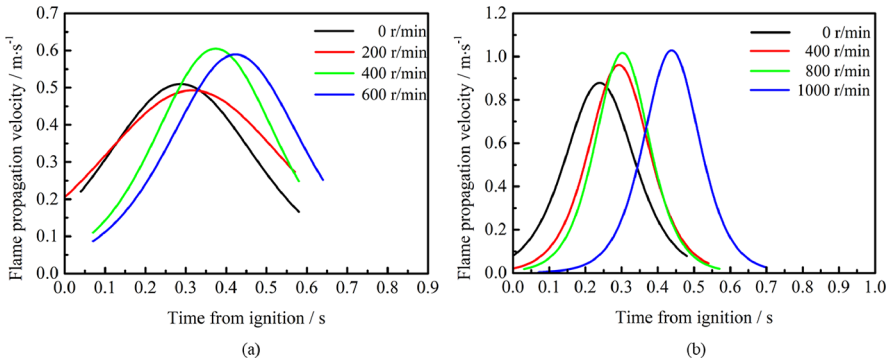


**Figure 9.** Variation of flame propagation speed with different speeds of the stirrer: (a) l0.0 and (b) 75.0%.

After analyzing the experimental data, the curves of the flame front and flame propagation velocity of the syngas were received, as presented in Figures 8 and 9. The flame propagation velocity had the same change trend under different initial turbulence intensities, all showing an inverted U-shaped parabola shape. It had experienced the process of accelerating first and then decelerating, which was consistent with the change law of other hydrocarbon fuels.[44−47] The flame front of syngas reached the maximum height at 500.0, 500.0, 560.0, and 560.0 ms under the test conditions of 0, 200.0, 400.0, and 600.0 r/min at an explosion concentration of 10.0%, respectively. The flame speeds reached the maximum at 286.0, 316.0, 374.0, and 423.0 ms after ignition, which were 0.510, 0.493, 0.605, and 0.589 m/s, respectively. At an explosion concentration of 75.0%, the flame front reached its maximum height at 460.0, 500.0, 490.0, and 630.0 ms under the test conditions of 0, 400.0, 800.0, and 1000 r/min, respectively. The flame speeds reached the maximum at 239.0, 292.0, 302.0, and 495.0 ms after ignition, which were 0.879, 0.961, 1.017, and 1.028 m/s, respectively. With the increase in rotating speed, the height of the flame front decreased and the maximum velocity of flame propagation increased.

The pulsation of turbulence promotes the bending and deformation of the burning flame surface, forms many folds, expands the reaction area, promotes the transportation of combustible substances and heat, and increases the upward propagation speed of the flame. However, the disturbance of turbulence also promotes the mixing and contact of the inert gas (nitrogen) in the syngas with the flame, which is not conducive to the spread of the flame. There is a competition mechanism between the positive effect of turbulence promoting the transport of combustible components and the negative effect of promoting the transport of inert components. In this study, the positive effect of turbulence on the transport of combustible components increased the maximum flame propagation velocity, while the negative effect of turbulence on the transport of inert components delayed the occurrence time of maximum flame propagation velocity. Therefore, with the increase in turbulence intensity, the maximum velocity of flame propagation increased, while the flame duration became longer.

**Table 5. Statistics of Syngas with Various Concentrations**

| syngas (vol %) | CO (vol %) | $H_2$ (vol %) | $N_2$ (vol %) | air (vol %) |
|---|---|---|---|---|
| 10.0 | 4 | 4 | 2 | 90.0 |
| 10.5 | 4.2 | 4.2 | 2.1 | 89.5 |
| 11.0 | 4.4 | 4.4 | 2.2 | 89.0 |
| 11.5 | 4.6 | 4.6 | 2.3 | 88.5 |
| 12.0 | 4.8 | 4.8 | 2.4 | 88.0 |
| 73.5 | 29.4 | 29.4 | 14.7 | 26.5 |
| 74.0 | 29.6 | 29.6 | 14.8 | 26.0 |
| 74.5 | 29.8 | 29.8 | 14.9 | 25.5 |
| 75.0 | 30 | 30 | 15 | 25.0 |
| 75.5 | 30.2 | 30.2 | 15.1 | 24.5 |

After the mixed gas was ignited, the flame front spread upward in a regular spherical shape. When the experiment was carried out at different rotating speeds, the stirrer rotated at a certain speed at the bottom of the reaction chamber, and the rotation of the stirrer drove the flow of gas from bottom to top. The gas flow direction was the same as the flame propagation direction, so the maximum flame propagation speed increased.

The analysis of the whole test results shows that after the premixed gas of syngas and air was ignited by electric spark, a


https://doi.org/10.1021/acsomega.1c02513
ACS Omega 2021, 6, 30910−30918

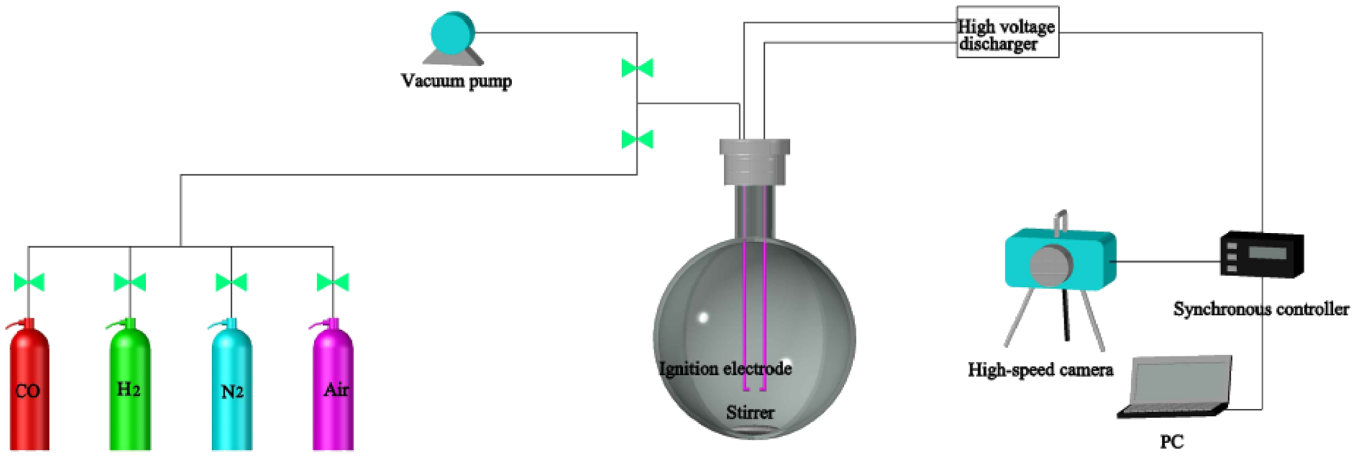


**Figure 10.** Schematic of the experimental system.

chemical reaction center was formed, which was the blue flame center visible in high-speed photography. The flame front spread in a regular spherical shape to the surroundings. The heat and active molecules in the center of the flame transferred energy to the unburned gas mixture around the flame through heat exchange and activation reaction. In the early stage of combustion, the flame propagation speed was slow. With the flame propagation, the spherical flame slowly expanded, and the flame propagation speed gradually increased. As the combustion reaction progresses, the concentration of the syngas gradually decreased, and the flame speed gradually decreased. The flame propagated forward with a regular spherical surface. With the increase in rotating speed, the flame shape changed obviously, there were many irregular folds on the flame surface, and the higher the speed, the more obvious the folds. When the rotating speed was different, the gas flow state was different, and the increase in rotating speed strengthened the disturbance to the flame propagation process, which made the flame front become an irregular toothed structure and present different folded surfaces. The maximum speed of flame propagation increased with the increase in turbulence.

## 3. CONCLUSIONS

In this paper, the effect of turbulence on the explosion limit and flame propagation process of syngas−air mixture was studied experimentally. The main conclusions are as follows:

(1) The explosion limit of syngas in the macro-static state was 9.5−76.1%. With the increase in turbulence intensity, both the upper and lower explosion limits decreased.

(2) In the macro-static state, the flame front was relatively smooth, and the flame propagation speed depicted a trend of first increasing and then decreasing. For syngas near the lower explosion limit, with the increase in concentration, the flame propagation speed increased obviously, and the flame duration decreased obviously. For syngas near the upper explosion limit, with the increase in concentration, the flame propagation speed decreased significantly, and the flame duration increased significantly.

(3) In the turbulent state, the flame front was wrinkled and the boundary was unclear. The larger the turbulence intensity was, the more obvious the fold of flame front was and the fuzzier the flame boundary was. With the increase in turbulence intensity, the flame duration became longer and the maximum speed of flame propagation increased.

## 4. EXPERIMENTAL SECTION

The statistics of syngas with various concentrations are summarized in Table 5. The gas explosion test system is shown in Figure 10. The test system consisted of an explosion limit tester (including an ignition system), gas distribution system, high-speed camera, and synchronous control system. The explosion limit tester was mainly composed of a glass pressure test container with a volume of 5.0 L and a stainless-steel host (heating furnace). The ignition electrode was placed in the test vessel with an electrode spacing of 6.4 mm and a high-voltage power supply of 15.0 kV/30.0 mA. In this study, the ignition duration of the electrodes was set to 400 ms. The egg-shaped magnetic stirrer with PTFE coating was placed in the glass test container, and the stirring speed could be set at 0−1200.0 r/min.

Before the test was started, the explosive vessel was pumped to create a vacuum. First, the three gases CO, $H_2$, and $N_2$ were injected into the test container in a fixed proportion to meet the pressure required for the test, and the air intake was adjusted by observing the pressure gauge reading. Then, the air was introduced into the test container slowly until the pressure in the container reached atmospheric pressure. Next, the magnetic stirrer was turned on and stirred for 5.0 min until the gas was evenly mixed. After the stirrer was turned off for 2.0 min (to ensure that the reaction chamber was in a macro-static state before ignition), the ignition of the electrode was completed by clicking the high-voltage discharge ignition button. If the explosion limit was tested at a certain stirring speed, then it was necessary to place it at the speed for 5.0 min (to ensure that it reached a stable turbulent state) before the ignition. In the ignition stage, the flame combustion process was recorded by the high-speed camera, which was synchronized with the ignition of the electrode by the control system. All the experiments were tested under room temperature (25.0−30.0 °C) and ambient pressure.

## AUTHOR INFORMATION

### Corresponding Authors

**Yingxin Tan** − *School of Environmental and Safety Engineering, North University of China, Taiyuan 030051, China*; Email: 13934240901@163.com

**Weiguo Cao** − *School of Environmental and Safety Engineering, North University of China, Taiyuan 030051, China*;



https://doi.org/10.1021/acsomega.1c02513
*ACS Omega* 2021, 6, 30910−30918

orcid.org/0000-0002-7058-561X; Email: cwgiem@163.com

### Authors

**Huarong Zhang** − *School of Environmental and Safety Engineering, North University of China, Taiyuan 030051, China*

**Shuo Zhang** − *School of Environmental and Safety Engineering, North University of China, Taiyuan 030051, China*

**Yabei Xu** − *School of Environmental and Safety Engineering, North University of China, Taiyuan 030051, China*

**Yuxin Zhao** − *School of Environmental and Safety Engineering, North University of China, Taiyuan 030051, China*

**Jiaxin Guo** − *School of Environmental and Safety Engineering, North University of China, Taiyuan 030051, China*

Complete contact information is available at: https://pubs.acs.org/10.1021/acsomega.1c02513

### Notes

The authors declare no competing financial interest.

## ■ ACKNOWLEDGMENTS

This work was supported by the Key Research and Development (R&D) Projects of Shanxi Province (grant no. 201903D121028) and the Platform Base and Outstanding Talent of Shanxi Province (grant no. 201705D211002).

## ■ REFERENCES

(1) Jiang, Y. H.; Li, G. X.; Li, H. M.; Zhang, G. P.; Lv, J. C. Experimental study on the influence of hydrogen fraction on self-acceleration of $H_2$/CO/air laminar premixed flame. *Int. J. Hydrogen Energy* **2020**, *45*, 2351−2359.

(2) Zhang, Y.; Chen, R.; Zhao, M.; Luo, J.; Feng, W.; Fan, W.; Tan, Y.; Cao, W.; Shu, C. M.; Yu, C. Hazard evaluation of explosion venting behaviours for premixed hydrogen-air fuels with different bursting pressures. *Fuel* **2020**, *268*, 117313.

(3) Li, D. J.; Xiao, Y.; Lu, H. F.; Xu, F.; Liu, K. H.; Shu, C. M. Effects of 1-butyl-3-methylimidazolium tetrafluoroborate on the exothermic and heat transfer characteristics of coal during low-temperature oxidation. *Fuel* **2020**, *273*, 117589.

(4) Yu, M.; Yang, X.; Zheng, K.; Zheng, L.; Wen, X. Experimental study of premixed syngas/air flame deflagration in a closed duct. *Int. J. Hydrogen Energy* **2018**, *43*, 13676−13686.

(5) Zhang, M.; Wang, J.; Chang, M.; Huang, Z. Turbulent flame topology and the wrinkled structure characteristics of high pressure syngas flames up to 1.0 Mpa. *Int. J. Hydrogen Energy* **2019**, *44*, 15973−15984.

(6) Cao, W.; Li, W.; Zhang, Y.; Zhou, Z.; Zhao, Y.; Yang, Z.; Liu, X.; Yu, S.; Tan, Y. Experimental study on the explosion behaviors of premixed syngas-air mixtures in ducts. *Int. J. Hydrogen Energy* **2021**, *46*, 23053−23066.

(7) Asgari, N.; Padak, B. Effect of fuel composition on NOx formation in high-pressure syngas/air combustion. *AIChE J.* **2018**, *64*, 3134−3140.

(8) Wang, P.; Guo, T.; Xu, H.; Zhao, Y.; Meng, S.; Feng, D.; Sun, S. Study on the effect of $H_2O$ on the formation of CO in the counterflow diffusion flame of $H_2$/CO syngas in $O_2$/$H_2O$. *Fuel* **2018**, *234*, 516−525.

(9) Canepa, E.; Nilberto, A. Experimental flame front characterisation in a lean premix burner operating with syngas simplified model fuel. *Energies* **2019**, *12*, 2377.

(10) Zhang, Y.; Cao, W.; Shu, C.-M.; Zhao, M.; Yu, C.; Xie, Z.; Liang, J.; Song, Z.; Cao, X. Dynamic hazard evaluation of explosion severity for premixed hydrogen−air mixtures in a spherical pressure vessel. *Fuel* **2020**, *261*, 116433.

(11) He, Y.; Wang, Z.; Weng, W.; Zhu, Y.; Zhou, J.; Cen, K. Effects of CO content on laminar burning velocity of typical syngas by heat flux method and kinetic modeling. *Int. J. Hydrogen Energy* **2014**, *39*, 9534−9544.

(12) Yu, M.; Luan, P.; Zheng, K.; Yang, X.; Han, S.; Duan, Y. Experimental study on explosion characteristics of syngas with different ignition positions and hydrogen fraction. *Int. J. Hydrogen Energy* **2019**, *44*, 15553−15564.

(13) Fu, P.; Zhang, A.; Luo, S.; Yi, W.; Hu, S.; Zhang, Y. Catalytic steam reforming of biomass-derived acetic acid over two supported Ni catalysts for hydrogen-rich syngas production. *RSC Adv.* **2019**, *4*, 13585−13593.

(14) Chen, J.; Chen, J.; Zhang, A.; Deng, H.; Wen, X.; Wang, F.; Sheng, W.; Zheng, H. Numerical simulation of the effect of $CH_4$/CO concentration on combustion characteristics of low calorific value syngas. *RSC Adv.* **2021**, *6*, 5754−5763.

(15) Gong, L.; Duan, Q.; Liu, J.; Li, M.; Li, P.; Jin, K.; Sun, J. Spontaneous ignition of high-pressure hydrogen during its sudden release into hydrogen/air mixtures. *Int. J. Hydrogen Energy* **2018**, *43*, 23558−23567.

(16) Li, P.; Duan, Q.; Gong, L.; Jin, K.; Chen, J.; Sun, J. Effects of obstacles inside the tube on the shock wave propagation and spontaneous ignition of high-pressure hydrogen. *Fuel* **2019**, *236*, 1586−1594.

(17) Cao, W.; Li, W.; Yu, S.; Zhang, Y.; Shu, C.-M.; Liu, Y.; Luo, J.; Bu, L.; Tan, Y. Explosion venting hazards of temperature effects and pressure characteristics for premixed hydrogen-air mixtures in a spherical container. *Fuel* **2021**, *290*, 120034.

(18) Cao, W.; Liu, Y.; Chen, R.; Li, W.; Zhang, Y.; Xu, S.; Cao, X.; Huang, Q.; Tan, Y. Pressure release characteristics of premixed hydrogen-air mixtures in an explosion venting device with duct. *Int. J. Hydrogen Energy* **2021**, *46*, 8810−8819.

(19) Olm, C.; Zsely, I. G.; Varga, T.; Curran, H. J.; Turanyi, T. Comparison of the performance of several recent syngas combustion mechanisms. *Combust. Flame* **2015**, *162*, 1793−1812.

(20) Tran, M. V.; Scribano, G.; Chong, C. T.; Ng, J. H.; Ho, T. X. Numerical and experimental study of the influence of $CO_2$ dilution on burning characteristics of syngas/air flame. *J. Energy Inst.* **2019**, *92*, 1379−1387.

(21) Varghese, R. J.; Kumar, S. Machine learning model to predict the laminar burning velocities of $H_2$/CO/$CH_4$/$CO_2$/$N_2$/air mixtures at high pressure and temperature conditions. *Int. J. Hydrogen Energy* **2020**, *45*, 3216−3232.

(22) Li, H. M.; Li, G. X.; Jiang, Y. H. Laminar burning velocities and flame instabilities of diluted $H_2$/CO/air mixtures under different hydrogen fractions. *Int. J. Hydrogen Energy* **2018**, *43*, 16344−16354.

(23) Varghese, R. J.; Kolekar, H.; Hariharan, H.; Kumar, S. Effect of CO content on laminar burning velocities of syngas−air premixed flames at elevated temperatures. *Fuel* **2018**, *214*, 144−153.

(24) Varghese, R. J.; Kolekar, H.; Kumar, S. Demarcation of reaction effects on laminar burning velocities of diluted syngas−air mixtures at elevated temperatures. *Int. J. Chem. Kinet.* **2019**, *51*, 95−104.

(25) Varghese, R. J.; Kolekar, H.; Kumar, S. Laminar burning velocities of $H_2$/CO/$CH_4$/$CO_2$/$N_2$ −air mixtures at elevated temperatures. *Int. J. Hydrogen Energy* **2019**, *2019*, 12188−12199.

(26) Wang, W.; Karatas, A. E.; Groth, C. P. T.; Gülder, O. L. Experimental and numerical study of laminar flame extinction for syngas and syngas-methane blends. *Combust. Sci. Technol.* **2018**, *190*, 1455−1471.

(27) Tran, M. V.; Scribano, G.; Chong, C. T.; Ho, T. X.; Huynh, T. C. Experimental and numerical investigation of explosive behavior of syngas/air mixtures. *Int. J. Hydrogen Energy* **2018**, *43*, 8152−8160.

(28) Liu, J.; Wang, J.; Zhang, N.; Zhao, H. On the explosion limit of syngas with $CO_2$ and $H_2O$ additions. *Int. J. Hydrogen Energy* **2018**, *43*, 3317−3329.

(29) Sun, Z. Y. Laminar explosion properties of syngas. *Combust. Sci. Technol.* **2020**, *192*, 166−181.

(30) Yang, S.; Saha, A.; Liang, W.; Wu, F.; Law, C. K. Extreme role of preferential diffusion in turbulent flame propagation. *Combust. Flame* **2018**, *188*, 498−504.

(31) Zhang, B.; Chang, X.; Bai, C. End-wall ignition of methane-air mixtures under the effects of $CO_2$/Ar/$N_2$ fluidic jets. *Fuel* **2020**, *270*, 117485.
(32) Scheid, M.; Geisler, A.; Krause, U. Experiments on the influence of pre−ignition turbulence on vented gas and dust explosions. *J. Loss Prev. Process Ind.* **2006**, *19*, 194−199.
(33) Wang, L.; Si, R.; Li, R.; Huo, Y. Experimental investigation of the propagation of deflagration flames in a horizontal underground channel containing obstacles. *Tunn. Undergr. Space Technol.* **2018**, *78*, 201−214.
(34) Wang, J.; Wu, Y.; Shan, W.; Zheng, L.; Pan, P.; Yu, M. Effect of Variable Cross−section Duct on Flame Propagation Characteristics of Premixed hydrogen/methane/air Combustible Gas. *Combust. Sci. Technol.* **2021**, *193*, 1425−1443.
(35) Starr, A.; Lee, J. H. S.; Ng, H. D. Detonation limits in rough walled tubes. *Proc. Combust. Inst.* **2015**, *35*, 1989−1996.
(36) Bauwens, C. R.; Dorofeev, S. B. Effect of initial turbulence on vented explosion overpressures from lean hydrogen−air deflagrations. *Int. J. Hydrogen Energy* **2014**, *39*, 20509−20515.
(37) Bai, C.; Chang, X.; Zhang, B. Impacts of turbulence on explosion characteristics of methane−air mixtures with different fuel concentration. *Fuel* **2020**, *271*, 117610.
(38) Sun, S.; Qiu, Y.; Xing, H.; Wang, M. Effects of concentration and initial turbulence on the vented explosion characteristics of methane−air mixtures. *Fuel* **2020**, *267*, 117103.
(39) Zhang, Q.; Liu, L.; Shen, S. Effect of turbulence on explosion of aluminum dust at various concentrations in air. *Powder Technol.* **2018**, *325*, 467−475.
(40) Zhang, X. Y.; Yu, J. L.; Sun, J. H.; Gao, W. Effects of turbulent intensity on nano−PMMA flame propagation behaviors. *J. Loss Prev. Process Ind.* **2016**, *44*, 119−124.
(41) Cao, W.; Qin, Q.; Cao, W.; Lan, Y.; Chen, T.; Xu, S.; Cao, X. Experimental and numerical studies on the explosion severities of coal dust/air mixtures in a 20-L spherical vessel. *Powder Technol.* **2017**, *310*, 17−23.
(42) Cheng, Y. F.; Su, J.; Liu, R.; Zan, W. T.; Zhang, B. B.; Hu, F. F.; Zhang, Q. W. Influential factors on the explosibility of the unpremixed hydrogen/magnesium dust. *Int. J. Hydrogen Energy* **2020**, *45*, 34185−34192.
(43) Wang, Z.; Meng, X.; Yan, K.; Ma, X.; Xiao, Q.; Wang, J.; Bai, J. Inhibition effects of $Al(OH)_3$ and $Mg(OH)_2$ on Al-Mg alloy dust explosion. *J. Loss Prev. Process Ind.* **2020**, *66*, 104206.
(44) Cao, W.; Li, W.; Zhang, L.; Chen, J.; Yu, S.; Zhou, Z.; Zhang, Y.; Shen, X.; Tan, Y. Flame characteristics of premixed $H_2$-air mixtures explosion venting in a spherical container through a duct. *Int. J. Hydrogen Energy* **2021**, 26693.
(45) Li, Y.; Bi, M.; Zhang, S.; Jiang, H.; Gan, B.; Gao, W. Dynamic couplings of hydrogen/air flame morphology and explosion pressure evolution in the spherical chamber. *Int. J. Hydrogen Energy* **2018**, *43*, 2503−2513.
(46) Zhang, Y.; Jiao, F.; Huang, Q.; Cao, W.; Shi, L.; Zhao, M.; Yu, C.; Nie, B.; Cao, X. Experimental and numerical studies on the closed and vented explosion behaviors of premixed methane-hydrogen/air mixtures. *Appl. Therm. Eng.* **2019**, *159*, 113907.
(47) Wang, Q.; Sun, Y.; Li, X.; Shu, C. M.; Wang, Z.; Jiang, J.; Zhang, M.; Cheng, F. Process of natural gas explosion in linked vessels with three structures obtained using numerical simulation. *Processes* **2020**, *8*, 52.


https://doi.org/10.1021/acsomega.1c02513
*ACS Omega* 2021, 6, 30910−30918